Vertical and horizontal resolution considerations for a joint 3D CSEM and MT inversion

Antony PRICE, Total E&P and Don WATTS, WesternGeco Electromagnetics*

Summary

To further explore the potential data content and inherent limitations of a detailed 3D Controlled Source ElectroMagnetic and MagnetoTelluric (CSEM+MT) dataset acquired over a known target, a constrained 3D CSEM and MT joint inversion (see Mackie, Watts and Rodi 2007) of these data is compared in detail with the known reservoir structure as derived from multiple well log and seismic data describing the physical properties (reservoir location and geometry etc.) of this hydrocarbon reservoir.

At the first order, individual channels and reservoir levels can be distinguished in the inverted electromagnetic (EM) data yielding a qualitative description of the stacked structure. Secondly, a more detailed and quantitative examination of the differences between the datasets reveals the measurement limitations and acquisition consequences (operational obstacles for the CSEM acquisition) of each of the datasets such as the resolution limits and inversion ambiguity of the EM data compared with the seismic and well logs. The goal of this paper is to better understand the reasons for the similarities and differences between these datasets in both the vertical and horizontal sense.

Introduction

The use of EM data for screening or exploration purposes has been well documented (see Constable and Weiss 2006 and Eidesmo and Ellingsrude 2002); however there appears to be a wealth of additional information contained in these data, particularly in datasets that have been acquired in a 3D grid pattern with relatively closely spaced receivers (of the order of 1-3 km). Further analysis of these data attempts to consider the limits of the horizontal and vertical resolution using 3D inversion of the EM data suitably constrained with the seismic depth horizons. These inversions initially took the form of simple and unconstrained 1D and 2D inversion of the CSEM data only, allowing definitive demonstration of detection using an electrical method. Work presented here demonstrates additional available information in the 3D CSEM and MT dataset in the form of a depth constrained inversion in 3D allowing for more complex geometries, multiple resistive horizons and a chance to examine the data at the reservoir scale.

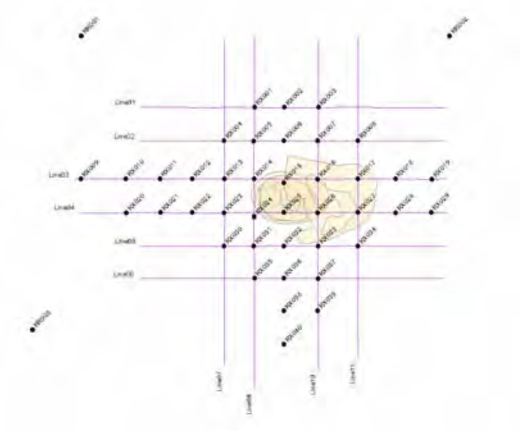

Figure 1: 3D CSEM+MT Acquisition layout with 43 receivers and 11 tow-lines. Note the absence of the central north-south tow-line due to an obstical. Reservoirs A-G displayed as poygons at the center.

The target examined here was chosen for a comprehensive 3D CSEM test as it is a complex and realistic structure for its setting in relatively deep water with a four-way closure and up to 6 symmetric and non-symmetric stacked reservoirs that offer an appropriate challenge for testing new technology and techniques such as CSEM acquisition, inversion and interpretation.

The survey acquisition design presented many challenges as seafloor receiver and transmitter tow-lines were required to respect exclusion zones for all current and future drilling and seabed infrastructure associated with the development of the field (see Figure 1). As a consequence, a central north-south tow-line was not acquired due to the presence of an active drilling rig, with consequences for the imaging of the shallowest reservoir discussed later. A dual frequency, time-share transmitter waveform of 0.25 and 0.0625 Hz was used to broaden the bandwidth and depth range of investigation with respect to the skin depth signal penetration limitations in a conductive environment. A majority of receivers were also equipped with vertical electrical sensors to measure the full vector compliment of the electric field.

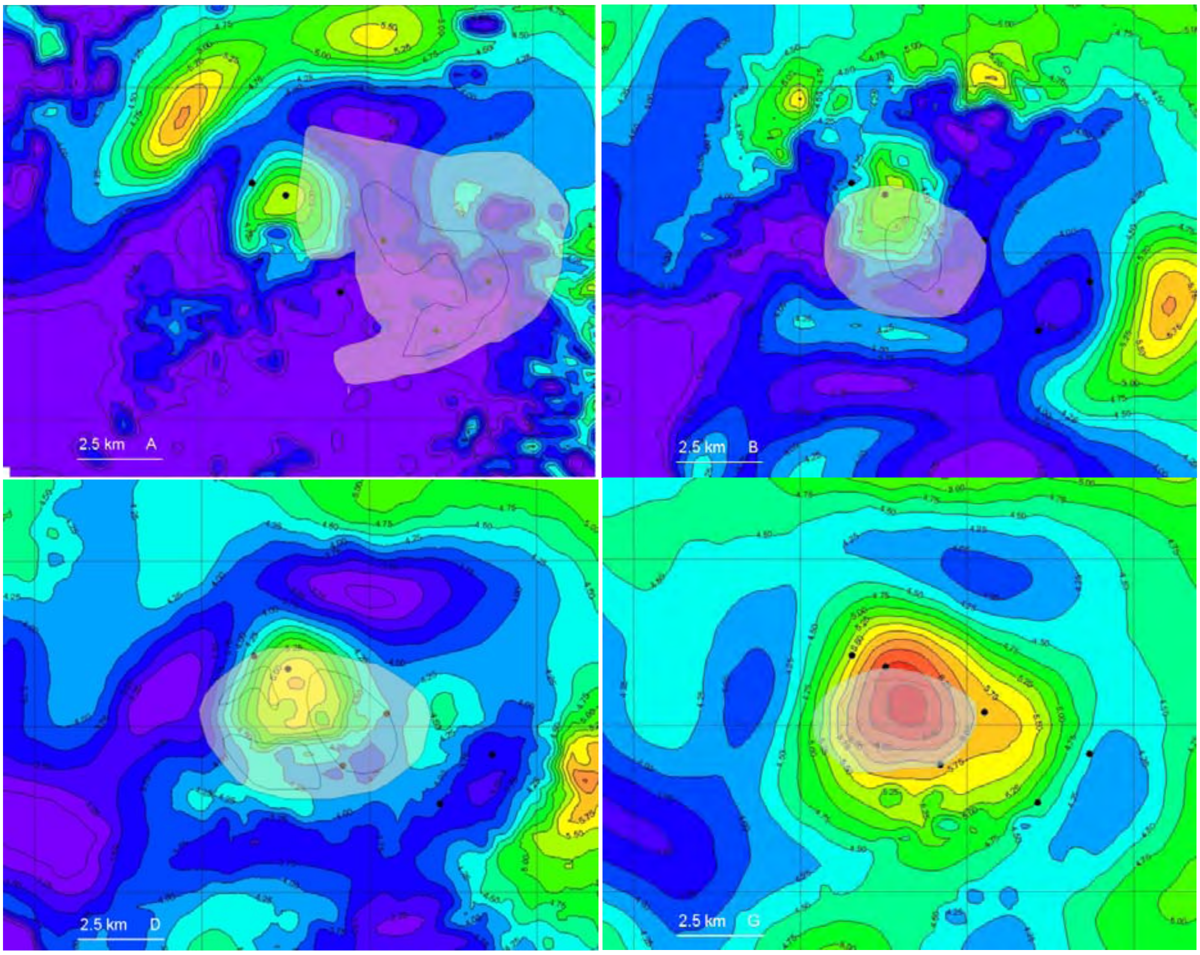

Figure 2: Individual reservoir seismic amplitude far offset (polygon overlays, A B D and G) describing the aerial reservoir distribution for four reservoir intervals over the equivalent interval joint 3D CSEM and MT inverted resistivity cube (contoured image). Important similarities and differences are clearly apparent.

Comparison with seismic estimates (Horizontal Resolution)

A standard exploration technique for identifying zones with the possible presence of hydrocarbons is to map the anomalous seismic amplitude at various offsets or angles over a restricted vertical range. Given the absence of the common complicating issues for seismic processing and imaging such as multiples, shallow gas/low velocity zones or complex structure, analysis of the amplitude and offset allows derivation of the acoustic impedance, Poisson's ratio and density in ideal conditions. Unfortunately the number of geological and fluid unknowns can exceed these derived parameters producing uncertainty or ambiguity in the interpretation. One example of such a difficulty is low gas saturation (fizz gas), for which the seismic technique has difficulty discriminating.

The application of resistivity derived from the inversion of EM data represents an independent parameter which can be interesting to compare with the reservoir and hydrocarbon distribution generated by the seismic and perhaps well information. Since resistivity can be more directly linked to saturation of hydrocarbons, it is a natural choice for increased fluid discrimination in conjunction with seismic data. For the purposes of this discussion we have considered the reservoir and fluid limits described by the seismic and well data to be the 'truth' against which we are

Figure 3: 3D CSEM+MT inversion E-W section constrained with seismic depth horizons for the reservoir levels. Note that the inversion is constrained vertically but not horizontally.

comparing the results from our CSEM+MT 3D inversion and analysis (represented as outlines over the EM inversions in Figure 2).

The differences in resolution and the gross location of the reservoirs seen by our joint CSEM+MT inversion and the seismic/well data is quite obvious (Figure 2, reservoir A, B and D), with the understanding that the 3D inverted EM data are loosely constrained in the vertical sense by the seismic depth horizons but not in the horizontal sense. The constraints here were established in the EM inversion as an a priori model constructed using the seismic horizons and resistivities from 1D inversions and well logs. The seismic horizons were included in the inversion as 'tear surfaces' which allow discontinuities in the regularization operator.

A possible explanation for the lateral discord between the acoustic and resistivity information is the EM inversion's tendency to fit the data with the simplest possible shape at the shallowest level given the seismic constraint. In addition the electrical imaging of the shallowest 'A' reservoir suffered due to the absence of the central transmitter tow-line mentioned earlier as a consequence of a rig obstacle at the time of acquisition. Sensitivity analysis supports this analysis, suggesting the absence of these data forced the reliance of the inversion on broadside information from the neighboring north-south lines which contain less information on vertical resistivity changes. Anisotropy was also examined as a potential convoluting factor in the inversion result; however this seemed not to be significant except for in the very shallow section (first 100's of meters). In addition, weighting of the CSEM and MT datasets in the inversion was evenly distributed (50/50) which may have biased the deeper structures against the shallower ones. A more illuminating and quantitative comparison between the EM data and the reservoirs could be made with additional horizontal constraint from the seismic acoustic data, or different weighting of the in-line and broadside EM data.

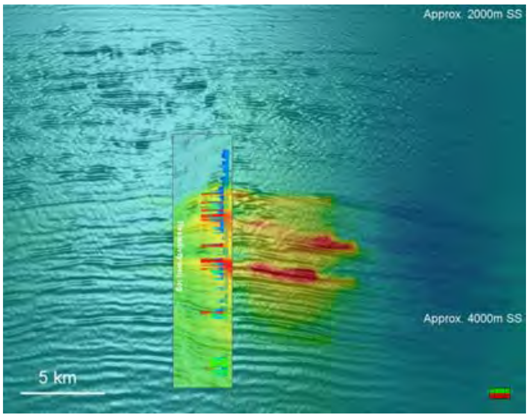

Figure 4: Direct comparison with constrained 3D CSEM+MT inversion E-W section and well resistivity log demonstrating general coherance between the two datasets.

Further work is underway to better quantify the differences and ascertain if they are solely inversion ambiguity or important differences in the separate physical properties measured by each technique.

Comparison with well resistivity data (Vertical Resolution)

For our dataset and target here, we can constrain the joint CSEM+MT inversion with key seismic horizons identified using amplitude analysis, allowing separation of the EM responses into their corresponding reservoir horizons. The inversion is constrained in the vertical sense but free in the horizontal direction testing the EM inversion's ability to isolate the known key reservoirs.

We know already that there are limitations to the lateral definition; however the vertical separation tells a potentially different story. An east-west section through the 3D resistivity cube of the constrained EM inversion is displayed in Figure 3 overlain on the corresponding seismic line with interesting lateral correlation with some of the brighter reflectors in the seismic data. Note that the strongest resistors suggesting the accumulations of hydrocarbons are not at the crest of the structure, which may demonstrate that some of the lateral asymmetry seen in Figure 3 is reflected in the resistivity inversions.

A more detailed comparison between the inverted EM data and the resistivity well log is seen in Figure 4 along the line displayed earlier. Note here that thinner resistive layers as seen by the well log are not resolved in the EM inversion due to their limited thickness demonstrating quite clearly the vertical resolution limits of the EM technique for this inversion approach.

Conclusions

The combination of several datasets should intuitively increase the confidence in the final interpretation. This is true of the gross representation of our target with the electrical technique of CSEM. These data do seem to contain information beyond those necessary for detection and possibly can inform us of the detailed structure of complex reservoirs. Differences remain however in the attempt to laterally define the individual reservoirs that are perhaps attributed to a variety of factors including inversion ambiguity and sensitivity that will require additional and perhaps more subtle constraint in the form of horizontal control derived from the seismic data.

We however have noted the possibility of the extended applications of EM data as seen here in the 3D joint CSEM+MT constrained inversion highlighting multiple reservoir levels. Clearly the inclusion of EM data and 3D inversion has increased the understanding of the use and limits of these data and will provide invaluable insights on how to use these data for future exploration, appraisal and possibly monitoring applications.

Acknowledgements

We would like to thank Total E&P for support and collaboration on this project and the kind permission to present the results of this test - in particular the affiliate for their extensive technical and logistic assistance, along with WesternGeco Electromagnetics for their role in acquisition, processing and interpretation of these data under often very difficult circumstances.

EDITED REFERENCES

Note: This reference list is a copy-edited version of the reference list submitted by the author. Reference lists for the 2009 SEG Technical Program Expanded Abstracts have been copy edited so that references provided with the online metadata for each paper will achieve a high degree of linking to cited sources that appear on the Web.

REFERENCES

Constable, S., and C. J. Weiss, 2006, Mapping thin resistor and hydrocarbons with marine EM methods: Insights from 1D modelling, Geophysics, **71**, no. 2, G43–G51.

Eidesmo T., S. Ellingsrud, L. M. MacGregor, S. Constable, M. C. Sinha, S. Johansen, F. N. Kong, and H. Westerdahl, 2002, Sea bed logging (SBL), a new method for remote and direct identification of hydrocarbon filled layers in deepwater areas: First Break, **20**, 144–152.

Ellingsrude, S., T. Eidesmo, S. Johansen, M. C. Sinha, L. M. MacGregor, and S. Constable, 2002, Remote sensing of hydrocarbon layers by seabed logging (SBL): Results from a cruise offshore Angola: The Leading Edge, **21**, 972–982.

Mackie, R., D. Watts, and W. Rodi, 2007, Joint 3D inversion of marine CSEM and MT data: 77th Annual International Meeting, SEG, Expanded Abstracts, 574–578.